Molecular Phylogenetics and Evolution 138 (2019) 31–42

Contents lists available at ScienceDirect

Molecular Phylogenetics and Evolution

journal homepage: www.elsevier.com/locate/ympev

Speciation with introgression: Phylogeography and systematics of the *Ameerega petersi* group (Dendrobatidae)

Connor M. French[a,1,*], Michael S. Deutsch[a], Germán Chávez[b], Carlos E. Almora[b], Jason L. Brown[a]

[a] Department of Zoology, Southern Illinois University, 1125 Lincoln Drive, Carbondale, IL 62901, USA
[b] División de Herpetología, Centro de Ornitología y Biodiversidad (CORBIDI), Santa Rita N°105 36 Of. 202, Urb. Huertos de San Antonio, Santiago de Surco, Lima, Peru

ARTICLE INFO

Keywords:
Phylogeography
Speciation
Frogs
Amazon
Introgression
Species tree

ABSTRACT

The Tropical Andes contains exceptionally high diversity, much of it arising within the Quaternary period. The complex geology of the Andes and paleoclimate fluctuations within the Quaternary suggest complex speciation scenarios. This, in turn, has contributed to idiosyncratic speciation modes among shallowly diverged Amazonian taxa. Many relationships among these taxa remain poorly resolved. Here we use a sequence capture approach, ultraconserved elements (UCEs), to address the phylogenetic relationships among three recently diverged Peruvian *Ameerega* poison frog species (*A. cainarachi, A. petersi,* and *A. smaragdina*; family Dendrobatidae) and explore a possible mode of speciation in this group. We assess concordance among concatenated phylogenetic tree inference, gene-tree based species tree inference, SNP-based species tree inference, and Bayes factor lineage delimitation to resolve species boundaries. We complement these analyses with assessments of call divergence to address the presence of a prezygotic reproductive barrier. Additionally, we further explore the phylogeographic history of these species of *Ameerega* with demographic inference, considering evidence for admixture and population expansions. Our results support the synonymy of *A. smaragdina* as a junior synonym of *A. petersi* and we find that speciation in this group is characterized by admixture and signatures of a population bottleneck followed by expansion. We invoke the disturbance-vicariance hypothesis to explain the observed patterns and call for more, detailed investigations of *in-situ* speciation in the Tropical Andes.

1. Introduction

Amazonia is the one of the primary sources of biodiversity in the Neotropics, yet how this biodiversity has accumulated remains poorly understood (Antonelli et al., 2018; Bush, 1994). Species richness is concentrated in western Amazonia, where it is presumed that the Andes have played a central role in its maintenance (Cheng et al., 2013; Hoorn et al., 2010). The transition zone between the Andes and lowland Amazonia, the Tropical Andes, is one of the most species-rich and threatened biodiversity hotspots in the world (Myers et al., 2000). A number of recent evolutionary radiations dating since the Miocene have occurred across the Tropical Andes; for example Godyrhidina butterflies (Chazot et al., 2016) and *Ameerega* poison frogs (Roberts et al., 2006, 2007).

These more recent *in-situ* diversification events could be driven by a number of mechanisms. Fluctuations in climate throughout the Pleistocene may have driven shifts in species distributions, isolating populations and resulting in allopatric speciation (Cheng et al., 2013; Colinvaux, 1987; Haffer, 1969). Under this scenario, the refugial hypothesis, allopatric species are expected to exhibit little to no gene flow, whereas in sympatric or parapatric populations it is expected to be higher. While there is some support for the refugial hypothesis in South America, for instance in Neotropical butterflies (Garzón-Orduña et al., 2014), most evidence suggests it does not explain the majority of South American diversity (da da Rocha and Kaefer, 2019). In topographically variable areas like the Tropical Andes, speciation histories may be complex, where repeated bouts of isolation and reconnection occur along elevational gradients before reproductive isolation is complete (Colinvaux, 1987, 1993). Bush (1994) proposed the disturbance-vicariance hypothesis to explain Andean and Amazonian diversity in light of Pleistocene climatic cycles. He argues that a combination of environmental factors, predominantly temperature and localized precipitation fluctuation, explain Amazonian diversity by influencing species dispersal from high-elevation Andean slopes to lowland Amazonian forests, tracking Pleistocene climatic fluctuations. Individual speciation histories of montane taxa are expected to exhibit traces of these cyclical

* Corresponding author.
E-mail addresses: cfrench@gradcenter.cuny.edu (C.M. French), michael.deutsch@siu.edu (M.S. Deutsch), jason.brown@siu.edu (J.L. Brown).
[1] Present address: Biology Department, The Graduate Center, City University of New York, 365 Fifth Avenue, New York, NY 10016, USA.

https://doi.org/10.1016/j.ympev.2019.05.021
Received 10 January 2019; Received in revised form 20 May 2019; Accepted 20 May 2019
Available online 22 May 2019

dynamics. Sympatric and parapatric species should demonstrate lower migration rates than expected based on their geographic proximity, while allopatric species show evidence of historical migration under this hypothesis (Noonan and Gaucher, 2005). Support has been demonstrated in frog species like the *Atelopus* toads (Noonan and Gaucher, 2005) and *Dendrobates* frogs (Noonan and Gaucher, 2006) whose demographic histories reflect a more dynamic speciation process than a single splitting event. In addition, there exists strong support for the complex speciation patterns predicted by the disturbance-vicariance hypothesis across a broad array of plant and animal taxa (Turchetto-Zolet et al., 2013).

The complex distributional history and large number of post-Miocene speciation events make the poison frog genus *Ameerega* (family Dendrobatidae) an ideal system to investigate speciation processes in the Tropical Andes. *Ameerega* is a radiation of poison frogs distributed along the Peruvian Tropical Andes into the Amazonian lowlands, with a few species reaching Brazil's Atlantic Forest (Santos et al., 2009). Their relatively recent origin (most recent common ancestor ~8.7 mya; Santos et al., 2009) and complex biogeography (Brown and Twomey, 2009; Roberts et al., 2007, 2006) is reflected by their constant taxonomic flux (Grant et al., 2017, 2006; Roberts et al., 2006; Santos et al., 2009).

Some groups are particularly problematic, such as the *Ameerega petersi* (=*Phyllobates petersi*, Silverstone, 1976) group, which consists of three common species distributed across the central and northern Peruvian foothills of the Andes in premontane and lowland rainforest (Brown and Twomey, 2009). A recent phylogenomic analysis of the genus places the *A. petersi* group as the sister taxon to *A. macero* (unpublished data, W.X. Guillory and J.L. Brown, 2018), although the most recent published phylogeny places them as the sister taxon to *A. simulans* (Santos et al., 2009). The three currently described species radiated recently (most recent common ancestor ~2.3 mya; Santos et al., 2009) and they span much of the elevational range of the foothills in the central cordilleras, reaching elevations of over 1300 m out of the cordilleras' ~2000 m peak height. All three species prefer sloped habitats rather than flat lowlands and depend on streams or nearby puddles for breeding. Two of the species, *A. petersi* and *A. smaragdina*, have overlapping distributions, while the third, *A. cainarachi*, is allopatric. *Ameerega petersi* and *A. smaragdina* are also phenotypically indistinguishable. The original diagnostic character between the two species, a smooth blue-green venter in *A. smaragdina*, has been observed in multiple genetically determined *A. petersi* populations, who typically have marbled blue-green venters (Brown and Twomey, 2009; Silverstone, 1976). No other morphological or behavioral differences have been reported for the two described species at either the adult or tadpole life stages. *Ameerega petersi* and *A. smaragdina* are consistently distinguishable from *A. cainarachi*, as follows: in advertisement calls (typical call consists of an irregular train of double, triple, and quadruple notes, or, only occasionally, in irregular trill vs. the call of *A. cainarachi* generally starts in an ascending series of notes culminating in an irregular trill); morphological differences in adults (*A. cainarachi* always possess a red dorsum with bright yellow dorsolateral lines vs. a black dorsum with green dorsolateral lines), and larvae (where the tip of tail possesses a pronounced upward curve in *A. cainarachi* and whose bodies are light brown vs. no curve in *A. petersi* whose bodies are black; Brown and Siu Ting, 2016). Lastly, populations of *A. cainarachi* are separated by more than 250 km from the closest known population of *A. petersi*.

However, mitochondrial DNA (mtDNA) data suggest three distinct lineages that correspond to the original proposed taxonomy by Silverstone (1976) (Brown and Twomey, 2009). Brown and Twomey (2009) explain this pattern, along with some geographic discontinuities in genetic lineages, by invoking a testable biogeographic hypothesis. They propose that repeated disturbance-vicariance events among weakly-differentiated ancestral populations led to mitochondrial introgression, obscuring present-day species relationships. Alternatively, Brown and Twomey's (2009) phylogeny may be the most likely hypothesis for the taxonomic relationships of the three species contained in the *A. petersi* group, and further investigation would be required to discover the reproductive isolating mechanisms between *A. petersi* and *A. smaragdina*. To address these hypotheses, we use genome-wide sequence capture data in the form of ultraconserved elements (UCEs). UCEs are able to resolve evolutionary relationships at shallow phylogenetic scales given their high sequence variation along the flanking regions of the loci, comparing favorably with other common genome-wide markers like restriction site associated DNA (RAD-seq) (Harvey et al., 2016). Therefore, we use UCEs to resolve the phylogenetic relationships and demographic histories of lineages in the *A. petersi* group. Specifically, we (i) test the specific status of *A. smaragdina* and *A. petersi* using lineage delimitation methods and call recordings, (ii) investigate the presence of genetic structure across their current distribution, and (iii) test for the presence of introgression between species and populations, which would be expected under the disturbance-vicariance model of speciation.

2. *Materials and* methods

2.1. Call analysis

Anuran species often have unique advertisement calls that are thought to act as reproductive barriers between closely related species (Boul et al., 2007). Therefore, we analyzed several aspects of frog call characteristics to investigate potential character displacement that indicates reproductive isolation between *A. petersi* and *A. smaragdina*. Male advertisement calls were recorded from December 11–14, 2016 (N = 3) and July 28–August 9, 2017 (N = 26). Since individual frog calls may vary with temperature, the ground temperature was measured at each calling site. Within *A. petersi* or *A. smaragdina* we observed substantial differences in call parameters between their train call and couplets (unpublished data MSD), thus measurements between the two call types are not analogous. Given the advertisement of *A. cainarachi* does not consist of a couplet of notes (rather a train of notes), we excluded them from our analyses. We focused call collection on two sites in forest habitats nearby the type localities of *Ameerega petersi* and *Ameerega smaragdina*: Alto Chivas (18.7 km from the *A. petersi* type locality, Pasco, Peru; 10.5095°S 74.91967° W) and Pan de Azucar (exact *A. smaragdina* type locality, near Iscozacin, Pasco, Peru; 10.24898° S 75.22558° W). The two localities are geographically proximate, separated by 56.2 km. Therefore–if *A. petersi* and *A. smaragdina* are distinct species–we expect their calls to be distinct in response to strengthened selective pressure for reproductive isolation.

Ameerega smaragdina and *A. petersi* have highly variable calls consisting of a continuous train of notes, and quadruple, triplet, and couplets of notes (Myers et al., 1998; Schlüter, 1980) that may influence the distribution of our measured call variables. Every surveyed population displays all call types and couplets are most common. Therefore, analyses were limited to "couplet" call patterns (Supplementary Fig. S1). The final dataset consisted of 13 calls and 16 calls of individuals of *A. smaragdina* and *A. petersi*, respectively. A single call recording was analyzed per individual. Five call variables were measured: dominant frequency (Hz), note duration (seconds), interval between notes (seconds), interval between couplets (seconds), and number of notes per second (Supplementary Fig. S1). Background noise was removed using the Noise Reduction tool in Audacity® 2.1.3 (https://audacityteam.org/). We analyzed eight consecutive notes per individual to ensure unbiased call variable estimates, selecting them from the center of calling bouts. The mean of each variable was used for further analysis. Seasonal effects were visually assessed at each step of the analysis and none were apparent. All call measurements were made in Raven 1.5 (Bioacoustics Research Program, 2014).

To reduce variable space, we first performed a scaled principal component analysis (PCA) on the five call variables. An analysis of

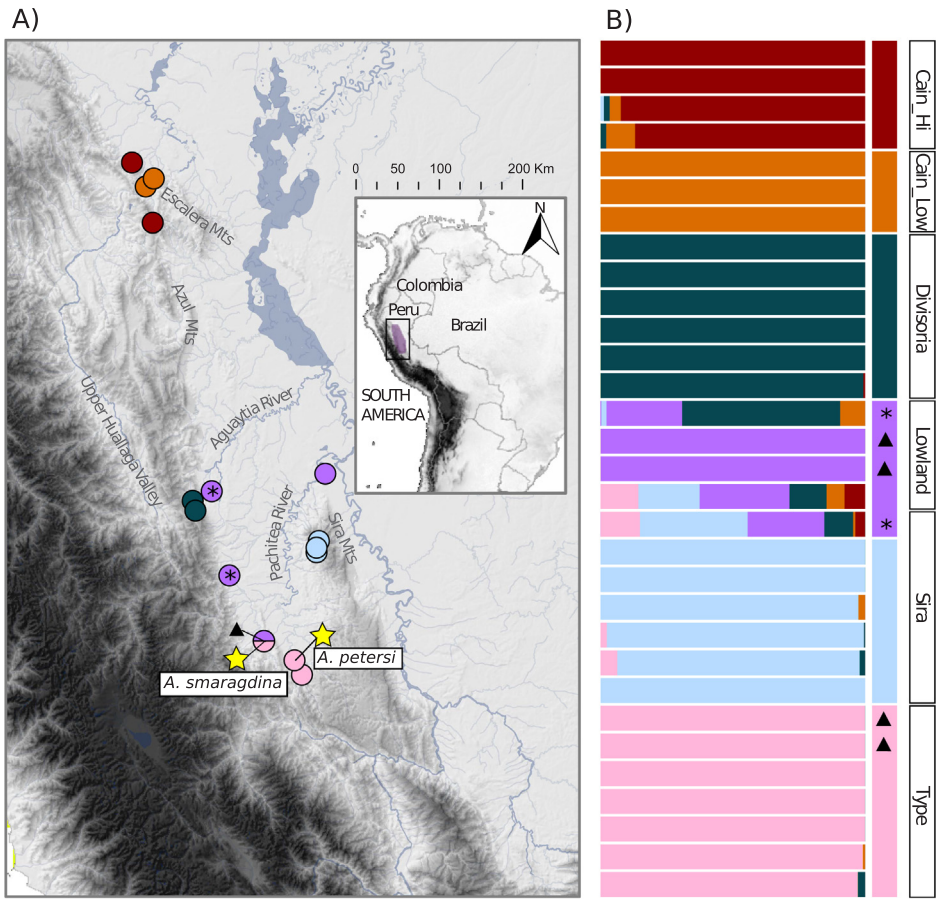

Fig. 1. The geographic distribution of genetic diversity in the *Ameerega petersi* group. A map of the Andean foothills of central Peru with genetic sampling localities (A). Colors correspond to populations inferred in an sNMF admixture analysis illustrated in (B), a barplot of ancestry coefficients with population assignments labeled. Populations are named according to geographically proximate landmarks– Cain_Hi (N = 4): High elevation *Ameerega cainarachi* population, Cain_Low (N = 3): Low elevation *A. cainarachi* population, Lowland (N = 5*): geographically dispersed mid- and low-elevation individuals, Divisoria (N = 6): Divisoria township, Sira (N = 6): El Sira Communal Reserve, Type (N = 7): near the type locality of *A. petersi*, except two *A. smaragdina* individuals collected from their respective type locality. Triangles indicate *A. smaragdina* individuals. All *A. smaragdina* were collected from their type locality. Asterisks indicate two individuals assigned to the Lowland population in a DAPC analysis, but not by sNMF. We classified these individuals as Lowland for species tree analysis and color them accordingly in the map. The half-shaded point in (A) indicates multiple populations inferred at the same locality. We denote localities where calls were recorded by stars and the species' name underneath. These localities also correspond to the species' type localities (in *A. petersi*'s case, a location less than 20 km away from the type locality).

variance (ANOVA) was performed on the first principal component as a continuous response and *species designation, temperature*, and *species designation*temperature* were used as predictor variables. A second ANOVA was conducted with PC2 as the response variable against the same predictor variables used in the first analysis. All analyses were completed with R version 3.3.2 (R Core Team 2016).

2.2. Tissue collection and sequencing

We sampled a total of 31 individuals from throughout the *A. petersi* group's range (Fig. 1; Supplementary Table S1). There were at least two individuals per species less than 20 km from the type localities of each species, including the two sites where calls were recorded. Repeated sampling along the Cordillera Azul at the juncture between *A. cainarachi* and *A. petersi*'s range turned up no individuals of either species (unpublished data, J. Brown, E. Twomey, and C.M. French 2003–2018), so we believe this to be true geographic separation. We used three individuals of the closely related species *A. macero* as the outgroup (Supplementary Table S1). Given the lack of morphological characters available to distinguish *A. petersi* and *A. smaragdina,* we designated *A. smaragdina* as only those individuals collected from their type locality. As *A. smaragdina* are only known from nearby their type locality, this effectively covers the known range of *A. smaragdina*. Tissue types included toe clips and tadpole tails, which were preserved in either 95% ethanol or a buffer solution of 20% DMSO saturated with sodium chloride and EDTA. We extracted genomic DNA using the Qiagen DNeasy Blood and Tissue Kit (Valencia, CA). We quantified DNA yield with a Qubit 3 fluorometer (ThermoFisher Scientific) and sent extracted DNA to RAPiD Genomics (Gainesville, FL, USA), where they performed sequence capture and Illumina sequencing of ultraconserved elements according to the UCE capture and sequencing protocols of Faircloth et al. (2012). Samples were enriched with a set of 5472 probes, targeting 5060 UCEs, using the Tetrapods-UCE-5Kv1 probe set (ultraconserved.org).

2.3. Sequence processing

The bioinformatics pipeline utilizes the PHYLUCE software package of python v2.7 scripts, with some modifications (Faircloth, 2016). We trimmed adapter contamination from raw reads with the *illumiprocessor.py* PHYLUCE script and then assembled trimmed reads using Trinity v2.0.6 (Grabherr et al., 2011). Reads were mapped to UCE loci using the *phyluce_assembly_match_contigs_to_probes.py* script, and basic read statistics were calculated using the *phyluce_assembly_get_fasta_lengths.py* script, the PHYLOCH V1.5–5 R software package, and custom scripts (Heibl 2008). We completed per-locus alignments and edge trimming in MAFFT, implemented with the *phyluce_align_seqcap_align.py* script (Katoh and Standley, 2013). Alignment summary statistics were calculated using the *phyluce_align_get_align_summary_data.py* script.

Using phased allele alignments rather than canonical nucleotide contigs increases the statistical power and accuracy of phylogenetic inference (Andermann et al., 2018). In addition, including allelic information conforms to the assumptions of the multi-species coalescent model (MSC), which is used by the species tree method used here (Zhang et al., 2017). We therefore followed Andermann et al. (2018)'s guidelines to obtain phased allele alignments. Briefly, we exploded the original FASTA alignment by each individual and used the resulting FASTA files as reference sequences for SNP calling. We then mapped cleaned reads to the individual reference libraries to obtain BAM pileups. The mapped reads were sorted and phased using the python script *phyluce_snp_phase_uces.py*, which utilizes *samtools* (Li et al., 2009). The phased sequences, now containing a reference allele sequence and alternative allele sequence for each individual, were aligned using

MAFFT. We retained sequences with at least 5 parsimony-informative sites and 75 percent of individuals present.

An alternative method to call SNPs for SNAPP and population structure inference was also used. A single individual of the closely related *A. macero* was used as the reference sequence. We first mapped UCE reads for each individual to the reference sequence using the program bwa v0.7.7 (Li and Durbin, 2009). PCR duplicates were marked using the program Picard v2.16.0. Variants were called with the Haplotype Caller tool in the Genome Analysis Toolkit v3.8.0 (GATK), which performs local realignment whenever it encounters a potential variant and negates the need to filter for indels (McKenna et al., 2010). Joint genotyping was performed using the GenotypeGVCFs tool in GATK. We filtered extracted SNPs using multiple thresholds: removing SNPs with a quality by depth less than 2.0, Fisher strand bias values greater than 60.0, mapping quality values less than 40.0, and mapping quality rank sum test score less than −12.5. We also hard-filtered each SNP to a depth of 8X. Only sites with no missing data were included, following the SNAPP program's guidelines. One SNP was randomly selected per UCE locus to minimize potential linkage disequilibrium. Summary statistics were calculated using the program vcftools (Danecek et al., 2011). We used two SNP data sets for downstream analysis: one that includes ingroup *A. petersi, A. smaragdina,* and *A. cainarachi* individuals and one that also includes outgroup *A. macero* individuals.

2.4. Genetic structure

The best-fit number of populations was inferred among *A. petersi, A. smaragdina,* and *A. cainarachi* using sNMF (Frichot et al., 2014). The sNMF algorithm uses sparse non-negative matrix factorization, a prior-free clustering algorithm, to compute regularized least-squares estimates of individual ancestry coefficients. When compared to other commonly-used algorithms used to estimate population ancestry (e.g. STRUCTURE, ADMIXTURE), sNMF performs with comparable accuracy, orders of magnitude faster (Frichot et al., 2014). A range of K values from 1 to 10 were tested with 50 replicates per K value. We ran the model with multiple alpha regularization parameter values (1, 10, 100, 1000) to assess the robustness of results to differing levels of model complexity. In addition to sNMF, we explored genetic structure with a discriminant analysis of principal components (DAPC), implemented in the R package adegenet v2.1.1 (Jombart, 2008; Jombart and Ahmed, 2011).

The demographic history of each population can inform assessments of the *A. petersi* group's biogeographic history. Therefore, the number of segregating sites and Watterson's theta (Watterson, 1975) were calculated to estimate within-population genetic diversity, and the neutrality statistics Tajima's D and Ramos-Onsins and Rozas' R_2 were calculated as measures of non-equilibrium demographic histories (Ramos-Onsins and Rozas, 2002; Tajima, 1989). P-values for the Tajima's D statistic were calculated by comparing the observed value against 1000 values simulated using the MS coalescent simulator (Hudson, 2002). All analyses were conducted in the R package PopGenome (Pfeifer et al., 2014).

2.5. Lineage delimitation

Bayes factor delimitation (BFD*) was used to compare support for six lineage delimitation hypotheses. BFD*, implemented as part of the BEAST software suite, uses a path sampling method to calculate marginal likelihoods for *a priori* species hypotheses (Leaché et al., 2014). Species hypotheses are then compared using Bayes factors (BF). Using this framework, we tested the original three-lineage *A. petersi, A. smaragdina,* and *A. cainarachi* hypothesis, a two-lineage (*A. petersi* + *A. smaragdina*) and *A. cainarachi* hypothesis, two hypotheses inferred from sNMF classifications, and two extensions of the sNMF classifications that constrain type-locality *A. smaragdina* individuals as a single lineage, opposing the most supported classifications (Table 2).

2.6. Phylogenetic and species tree inference

A maximum likelihood (ML) analysis was conducted using the concatenated UCE loci with the program IQ-TREE (Nguyen et al., 2015). We used ModelFinder to select the best-fit partition model (Kalyaanamoorthy et al., 2017) and ran 1000 ultrafast bootstrap replicates (Hoang et al., 2018). For ultrafast bootstrap replicates, a node is considered strong if it has 95 percent support. We also ran 1000 replicates of the SH-aLRT test, which can be interpreted similarly to the traditional bootstrap metric (Guindon et al., 2010). We used the -allnni option to conduct a more thorough search of tree space, searching all possible nearest-neighbor interchanges (NNI), rather than those in the vicinity of another NNI. We ran the analysis twice to ensure consistent results.

In addition to concatenated analysis, we inferred species trees using two methods based on the multispecies coalescent, ASTRAL-III v5.5.9 (Sayyari and Mirarab, 2016; Zhang et al., 2017) and SNAPP (Bryant et al., 2012). ASTRAL-III is a quartet-based method that samples individual gene trees to infer an unrooted species tree. We inferred gene trees with IQ-TREE, using ModelFinder to select best-fit substitution models and ran 1000 ultrafast bootstrap replicates for each UCE locus (Hoang et al., 2018; Kalyaanamoorthy et al., 2017). We ran ASTRAL-III with the resulting gene trees, using default parameters. SNAPP is a Bayesian species tree method, which uses biallelic SNPs to infer a species tree by integrating over all possible gene trees (Bryant et al., 2012). SNAPP is advantageous because large, complete matrices of unlinked SNPs are readily obtainable from UCE datasets. In addition, the SNAPP algorithm allows for population mutation rates (theta) to vary across populations, while other species tree methods make the unlikely assumption that theta is fixed. Forward and reverse mutation rates were calculated from the data set and the coalescence rate was sampled using a starting value of 27.0 determined from preliminary analyses, which converged near this value under different prior settings. Only polymorphic sites were used in our SNAPP analysis. The lambda prior was set to a gamma distribution with an alpha value of 2.0 and beta value of 20.0, with a median of 33.6 after testing a variety of shape parameters for appropriate convergence and mixing. We sampled the rate prior from a gamma distribution and used default values for all other parameters and set the MCMC chain length to two million generations, storing every 1000. At least two independent runs were conducted until convergences were achieved, which we assessed in Tracer V1.6 (http://tree.bio.ed.ac.uk/software/tracer/). We ran this procedure with the outgroup SNP data set.

2.7. Gene flow and reticulate evolution

Population splitting and mixing were inferred using the program TreeMix v1.13 (Pickrell and Pritchard, 2012). The method uses a graph-based approach to model population histories, allowing for population ancestry to include multiple parental populations (Pickrell and Pritchard, 2012). It first infers a maximum-likelihood tree of population relationships and builds a residual covariance matrix to assess model fit. Drift between an ancestral population and a focal population is estimated under a Gaussian model outlined in Cavalli-Sforza and Edwards (1967). Migration edges are added to pairs of populations with the largest residuals and the graph is optimized for branch lengths and the weight of the migration edge. The weight of a migration edge is the fraction of alleles inherited from one parental population relative to another, where the largest weight is considered the non-migration edge and the smallest weight is the migration edge. This process is repeated until the migration edge that improves the likelihood the most is chosen and is repeated for the total number of migration edges under consideration. Migration edge significance is estimated through a resampling procedure that quantifies the improvement in model fit of adding

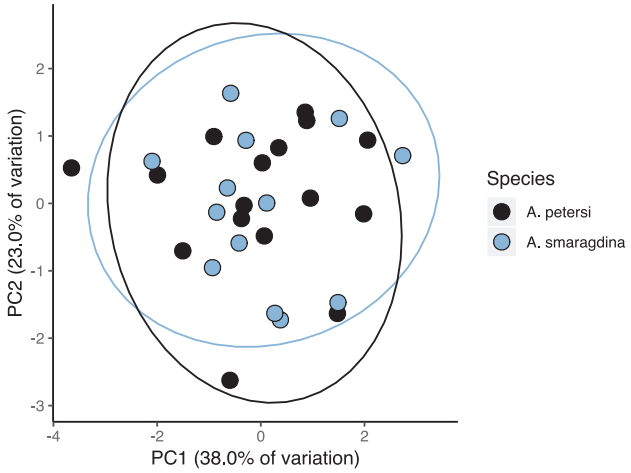

Fig. 2. First two principal component axes from a principal component analysis of five call variables. The five variables include dominant frequency (Hz), note length (s), space between notes (s), space between pulses (s), and call rate (calls/s). Ellipses represent 95% confidence intervals.

a new migration edge with its corresponding weight relative to uncertainty in migration weight estimation across the genome. Positive values of the residual covariance matrix indicate pairs of populations where the model underestimates their covariance, implying that adding more branches may improve model fit. Negative residuals indicate overestimation of population pair covariance, implying that there may be unmodeled migration elsewhere in the graph. The outgroup SNP data set was used and we allowed from zero to three migration edges in consecutive analyses. In addition to the migration edges inferred by TreeMix, we calculated the less-parameterized three population (f_3) and four population (f_4) tests for a robust inference of admixture (Reich et al., 2009). The tests detect correlations in allele frequencies that do not conform to a bifurcating model of population evolution (Reich et al., 2009).

3. Results

3.1. Call analysis

The first and second principal components (PCs) of call variables explained 61.0 percent of the total variation in the call data set (Fig. 2; see Supplementary Table S2 for variable loadings). Species designation ($P = 0.852$; $F = 0.036$), temperature ($P = 0.082$; $F = 3.292$), and the interaction between species designation and temperature ($P = 0.658$; $F = 0.201$) did not significantly explain PC1 in an ANOVA. None of the explanatory variables significantly explained PC2 (all $P > 0.50$). There is no quantifiable divergence in the observed call parameters between *A. petersi* and *A. smaragdina*.

3.2. UCE sequencing

A total of 2340 loci were recovered across all individuals. After filtering for loci that contain at least 75 percent of individuals, we recovered 1061 loci. Low-variation loci can negatively impact

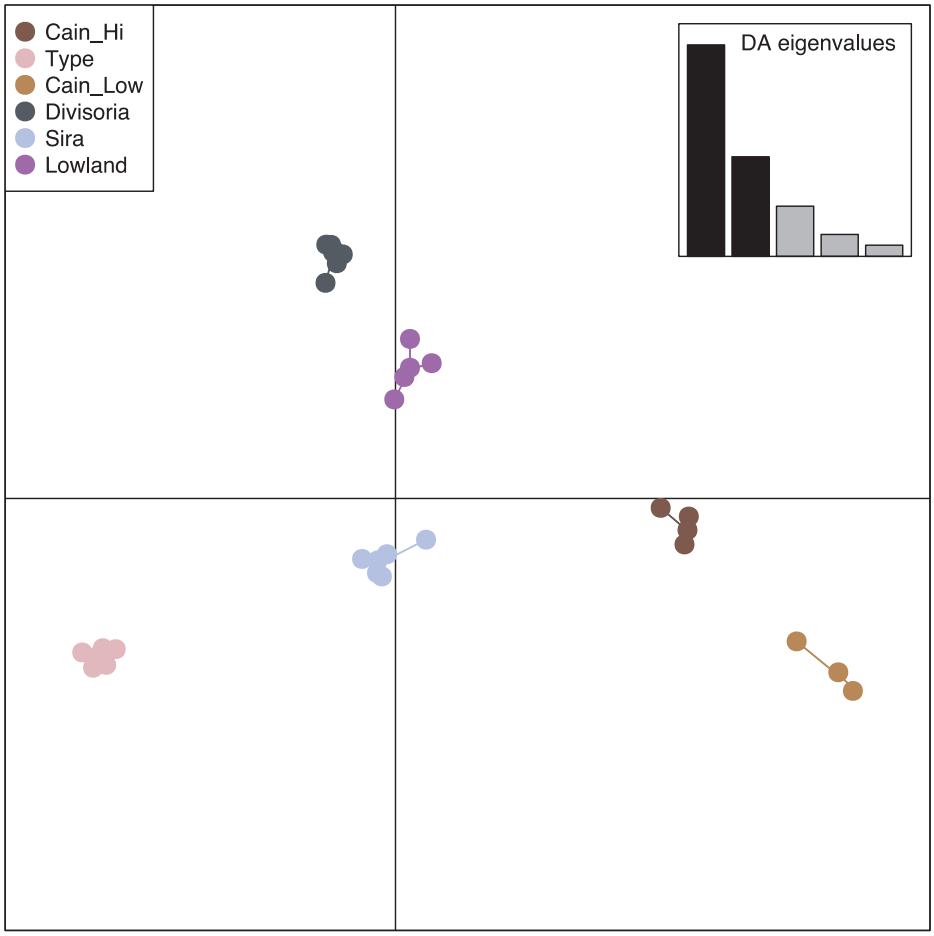

Fig. 3. Discriminant analysis of principal components (DAPC) plot of unlinked SNPs. Colors correspond to those in the sNMF analysis (Fig. 1). Inset is a plot of the relative percent variation explained by each of the retained discriminant analysis (DA) eigenvectors.

phylogenetic inference and summary-based species tree methods (Hosner et al., 2016; Manthey et al., 2016). Therefore, we filtered for loci with greater than or equal to 5 parsimony-informative sites (PIS), a threshold determined to produce consistent results (Hosner et al., 2016). We retained 618 loci with an average length of 488.995 base pairs and a range from 227 to 952 bp ("full" data set). The average number of PIS across loci was 10.968, ranging from 5 to 41 PIS. Under the alternative SNP-calling strategy, 1206 SNPs were retained after filtering for no missing data and limiting to one random SNP per locus ("full" data set). A subset of this data set limited to ingroup individuals ("ingroup") was produced for sNMF analysis (1031 SNPs).

3.3. Genetic structure

Six populations (*K*) were recovered by the sNMF analysis and DAPC analysis of the ingroup SNP data set (alpha = 100; cross-entropy = 0.312; Figs. 1 and 3). *Ameerega cainarachi* was recovered as two distinct populations, "Cain_Hi" and "Cain_Low", distinguished by the elevational differences between the two populations. *Ameerega petersi* was split into four populations. We classified three of the populations as "Type", "Sira", and "Divisoria" based on the individual's geographic proximity to the *A. petersi* type locality, El Sira Communal Reserve, and Divisoria township, respectively. A fourth population, "Lowland", was distributed incongruently across the range, consistently at lower elevations than the other *A. petersi* populations (Fig. 1).

The sNMF and DAPC analyses differed slightly in their population assignments. The DAPC clustering placed two admixed individuals assigned to the Sira and Divisoria populations, to the Lowland population (Fig. 3, indicated by asterisks in Fig. 1). Given the lowland distribution of the two individuals and strong differentiation based on the DAPC analysis, we included them in the Lowland population for lineage delimitation analysis.

Additionally, four *Ameerega smaragdina* individuals sampled from the type locality were assigned to two *A. petersi* populations. A *K* of 4 had the second-best cross-entropy score and lumped the Lowland population with Sira, except for one individual geographically proximate to Divisoria. The lumped individuals had heterogeneous admixture proportions across populations (Supplementary Fig. S2).

The Lowland and Type *A. petersi* populations, which occupy low and mid-elevation slopes, have higher intra-population genetic diversity than the more high-elevation populations (Table 1). In addition, Ramos-Onsins and Rozas' R_2 is below 0.10 for the Lowland (R_2 = 0.092) and Type (R_2 = 0.081) *A. petersi* populations, indicating support for a population bottleneck followed by range expansion (Ramos-Onsins and Rozas, 2002). Tajima's D statistics for the Lowland (D = −1.28, *P* = 0.102) and Type (D = −1.307, P = 0.075) populations are more negative than *A. cainarachi* and higher-elevation *A. petersi* populations, although they are not statistically significant at an alpha value of 0.05 (Table 1). This indicates some support for a demographic shift in the past among lower-elevation *A. petersi* populations, although statistical significance was not achieved.

Table 1
Genetic diversity and neutrality statistics for the 6-lineage hypothesis show evidence for non-equilibrium histories among some lineages. S indicates the number of segregating sites. P-values are associated with the Tajima's D test for neutrality.

Population	Watterson's theta	S	Rozas' R_2	Tajima's D	P-value
Cain_Hi	61.752	141	0.171	0.285	0.541
Cain_Low	63.251	164	0.135	−0.262	0.35
Divisoria	39.074	118	0.135	−0.014	0.432
Lowland	106.4	301	0.092	−1.28	0.102
Sira	75.831	229	0.107	−0.691	0.193
Type	80.814	257	0.081	−1.307	0.075

3.4. Lineage delimitation

The 6-lineage hypothesis without *A. smaragdina* was decisively favored over the original 3-lineage hypothesis (2 * ln(BF) = 14.476; Table 2). In addition, the original sNMF assignments (K = 4; K = 6) were supported over constraining *A. smaragdina* to be monophyletic (Table 2). Both of these results support the hypothesis that *A. smaragdina* is not a distinct evolutionary lineage.

3.5. Phylogenetic analysis and species tree inference

The concatenated ML analysis conducted in IQ-TREE supports consolidating *A. smaragdina* and *A. petersi* (lnL = −554130.492; Fig. 4; see Supplementary Fig. 3 for expanded phylogeny). The topology agrees with the population structure recovered in the sNMF analysis. However, individuals considered admixed by sNMF analysis receive low nodal support in the phylogeny, including the Lowland population (Fig. 4). *Ameerega cainarachi* was recovered as the sister taxon to *A. petersi*. Of note, nearly all phased allele pairs were recovered as sister taxa (excepting two *A. cainarachi* individuals, see Supplementary Fig. 3). This indicates that allelic variation is conserved within individuals.

Species assignments were made according to the *K* = 6 populations inferred by sNMF and DAPC analyses. The ASTRAL-III species tree topology suggests that *Ameerega cainarachi* forms a polytomy with the Divisoria population of *A. petersi* and a clade comprising the other three *A. petersi* populations (Fig. 5). The SNAPP species tree topology places two *A. petersi* populations (Divisoria and Lowland) as the sister group to *A. cainarachi*, with the Sira and Type *A. petersi* populations forming the sister group to the rest (Fig. 5B).

3.6. Gene flow and reticulate evolution

The TreeMix topology with no migration edges agreed with the ASTRAL-III topology (Fig. 6). The model that best fit the data supported three migration edges (Fig. 6). Adding more edges did not improve model support. The topology supported *A. petersi* and *A. cainarachi* as independent lineages, with two migration events between *A. cainarachi* and *A. petersi*. A third, non-significant migration event was inferred between *A. petersi* and *A. macero*, the outgroup. One migration edge connecting the Divisoria and Cain_Hi populations was statistically significant (*P* = 0.021). A migration event between the branch leading to the Divisoria and Lowland populations and the Cain_Low population approached significance (*P* = 0.086), while a migration event between the Type locality and *A. macero* was non-significant (*P* = 0.142). None of the migration events were supported by f_3 (all z-scores > −0.50) or f_4 (all z-scores between −1.0 and 1.0) tests. This, combined with sNMF results, indicates some support for admixture between species.

3.7. New synonymy

Ameerega petersi Silverstone, 1976

Dendrobates trivittatus Cochran and Goin, 1970, (partim): p 16.
Phyllobates petersi Silverstone, 1976 (partim): p 37–38. Fig. 2.
Phyllobates smaragdinus Silverstone, 1976: p 44-45. Fig. 2, Weygoldt, 1987.
Dendrobates petersi. Myers et al., 1978 (partin): p.33; Myers et al., 1998, p.1-20; Toft, 1980; Toft and Duellman, 1979; Duellman and Toft, 1979; Aichinger, 1987.
Epipedobates petersi. Myers, 1987 (partin): p. 303; Lötters et al., 2003; Rodríguez and Myers, 1993; Hödl, 1990; Aichinger, 1991, 1992.
Epipedobates smaragdinus Myers 1987: p. 303; Roberts et al., 2006, p. 4–8.
Ameerega petersi. Bauer, 1988 (partin): Frost et al., 2006 (partin); Grant et al., 2006 (partin), Lötters and Mutschmann, 2007 (partin);

Table 2
Bayes factor delimitation (BFD) results for six different lineage hypotheses. The most supported hypothesis is the six-lineage hypothesis. The first hypothesis is the original lineage hypothesis based on the current taxonomy. ML = marginal likelihood estimate, BF = Bayes factor, 2 * ln(BF) is a transformation to enable accurate comparison among models. The asterisk refers to a single Lowland individual assigned to the Divisoria population in the K = 4 sNMF analysis.

Model	Rank	ML	BF	2 * ln(BF)
(A. petersi)(A. smaragdina)(A. cainarachi)	5	−11950.66	0	–
(A. petersi, A. smaragdina)(A. cainarachi)	6	−12071.688	−121.028	−9.592
(Cain_Hi, Cain_Low)(Sira, Lowland)(Divisoria, Lowland*)(Type)	3	−10910.192	1040.468	13.895
(Cain_Hi)(Cain_Low)(Divisoria)(Lowland)(Sira)(Type)	1	−10559.094	1391.566	14.476
(Cain_Hi)(Cain_Low)(Divisoria)(Lowland)(Sira)(Type)(*A. smaragdina*)	2	−10592.059	1358.601	14.428
(Cain_Hi, Cain_Low)(Divisoria)(Sira, Lowland*)(Type)(*A. smaragdina*)	4	−11174.001	776.659	13.310

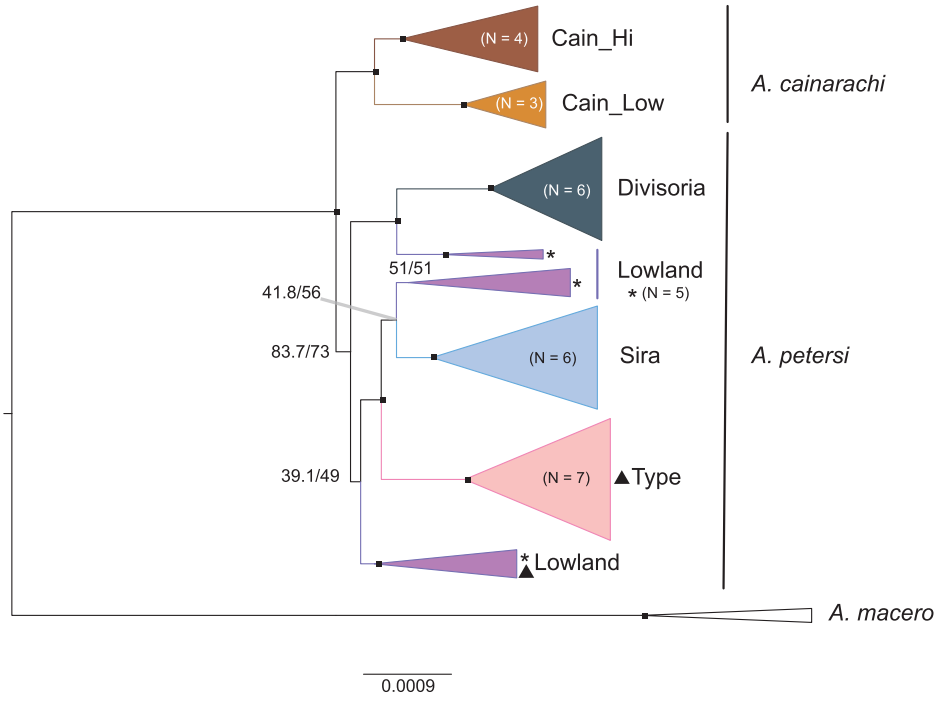

Fig. 4. Concatenated maximum likelihood phylogeny of the *A. petersi* group. Nodes are collapsed and colored according to the populations inferred in an sNMF analysis for clarity. Branch annotations are ultrafast bootstrap/SH-aLRT nodal support values. Dots indicate clades with ultrafast bootstrap scores ≥ 90 and SH-aLRt scores ≥ 80. Triangles indicate clades that contain *A. smaragdina* individuals (N = 2 for each clade).

Brown and Twomey, 2009; Amézquita et al., 2011; Serrano-Rojas et al., 2017.

Ameerega smaragdina Bauer, 1988: Frost et al., 2006; Grant et al., 2006, Lötters and Mutschmann, 2007; Brown and Twomey, 2009

On the basis of the molecular and behavioral evidence presented here, we consider *Ameerega smaragdina* (Silverstone, 1976) as a junior synonym of the more widespread species, *Ameerega petersi* (Silverstone, 1976) (see discussion for more information).

3.8. Definition and diagnosis

Ameerega petersi is assigned to the genus *Ameerega* on the basis of the following: first finger longer than second, webbing absent between the toes, dorsal skin granular (Myers, 1982, Grant et al., 2006). This is a medium species of *Ameerega* with an adult SVL of approximately 23.3–30.3 mm. Dorsum granular and dark-brown medially, black laterally; bright yellowish-green dorsolateral stripes extending from loreal region to groin. Bright yellowish-green labial stripe present starting behind nares and terminating above forelimb as a yellow patch. Yellow spots present and distinct above groin. Venter variable, yellow, green to sky-blue on black ground color, occasionally with black marbling. Teeth present. Appressed first finger longer than second; finger discs weakly expanded; hands and feet lacking webbing between digits. Vocalization consists of a series of irregularly-spaced notes in double, triple, and quadruples, and occasionally irregular trill notes occurring with a dominant frequency of 3500 Hz.

4. Discussion

4.1. Lineage delimitation and systematics of the Ameerega petersi group

Many dendrobatids exhibit extensive levels of intraspecific variation, making diagnoses based on a single coloration characteristic unstable (Rojas and Endler, 2013; Twomey et al., 2016). Supporting this, *Ameerega smaragdina*'s diagnosing phenotype, a lack of ventral marbling coloration, characterizes individuals with an *A. petersi* mtDNA haplotype (Brown and Twomey, 2009). In addition, *A. smaragdina's* distribution overlaps extensively with *A. petersi*'s and both species' vocalization patterns are variable enough to encapsulate variation seen in both species (Brown and Twomey, 2009; Myers et al., 1998; Silverstone, 1976). Therefore, we consider specific status of *Ameerega smaragdina* as invalid.

We provide multiple sources of evidence in support of this hypothesis. Reproductive character displacement should occur where species come back into contact (Lemmon, 2009; Liou and Price, 1994). The type localities of *A. petersi* and *A. smaragdina* are geographically proximate (Fig. 1; Silverstone, 1976), where call divergence should be strongest. We found no difference in a multivariate summary of five calling variables between individuals from the type locality of *A. smaragdina* and individuals near the type locality of *A. petersi* (Fig. 2). This is in contrast with other studies of anuran speciation, where geographic proximity is associated with strong call divergence (Boul et al., 2007; Lemmon, 2009).

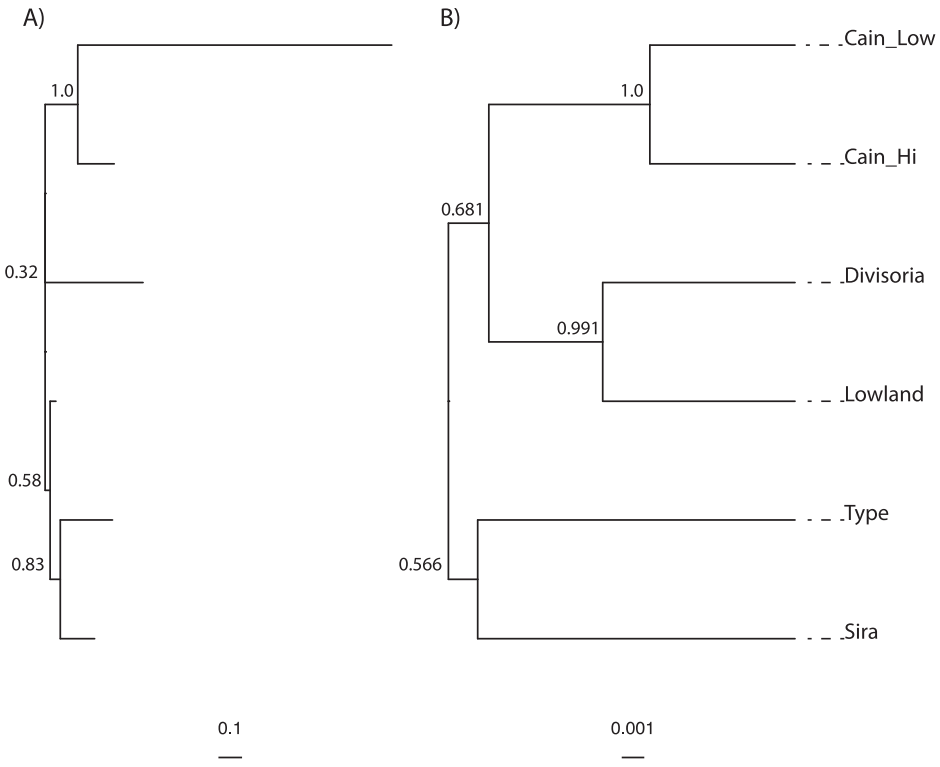

Fig. 5. ASTRAL-III and SNAPP species trees following the 6-lineage hypothesis. Tips are aligned vertically so tip labels are common between trees. Branch labels for the ASTRAL-III tree, (A) are local posterior probabilities. Branch labels for the SNAPP tree, (B) are posterior probabilities. The outgroup is omitted for clarity; both root nodes received full support.

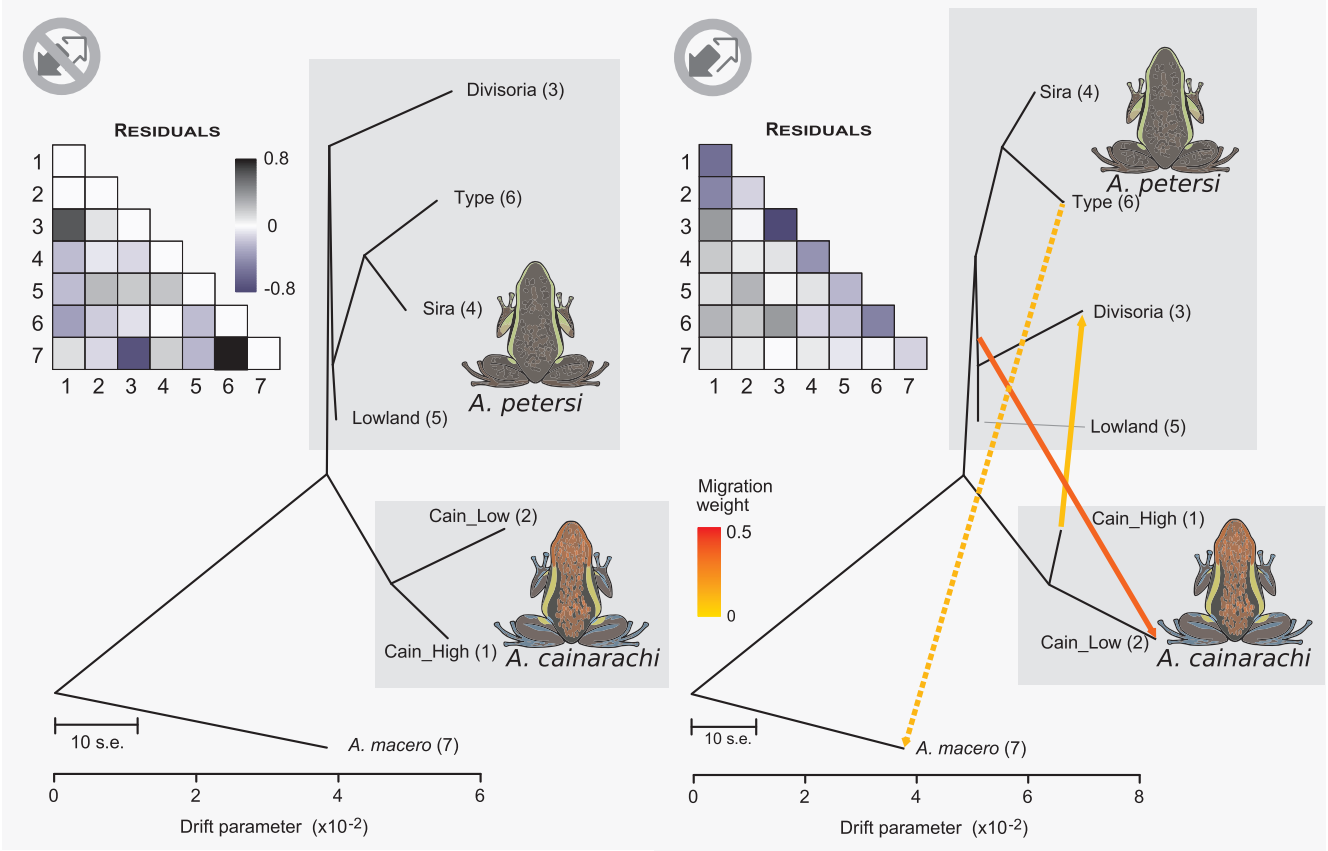

Fig. 6. TreeMix inference of population relationships and introgression. The yellow-red color scale indicates the weight of the migration edges. The drift parameter is a relative temporal measurement. The scale bar represents ten times the standard error of the allele frequency variance-covariance matrix. **Left.** The topology with zero migration edges. **Right.** The topology with three migration edges. Half-matrices depict heat maps of the model residuals for topologies. Darker colors indicate increased model uncertainty. The dashed migration edge vector depicts no statistical significance. Frog drawings: Wilson X Guillory.

In addition to a lack of evidence for behavioral reproductive isolation, we provide evidence from multiple analyses of UCE data that *A. smaragdina* is part of *A. petersi*. First, estimates of ancestry coefficients (sNMF) and a genetic clustering algorithm (DAPC) do not recover four individuals of *A. smaragdina* collected from their type locality as monophyletic (Figs. 1 and 3, Supplementary Fig. S2). The individuals are assigned to two populations, the Type and Lowland populations. Second, maximum likelihood phylogenetic analysis of a concatenated UCE matrix recovered the four *A. smaragdina* individuals as distributed across *A. petersi* populations (Fig. 4; Supplementary Fig. 3). To reconcile both species to represent clades would require the designation of several new taxa currently considered populations of *A. petersi*- something that makes little biological sense. Our maximum likelihood phylogeny recovered two *A. smaragdina* individuals as the sister group to the Sira and Type clades, although there is extremely weak support for the relationship (BS = 49). Finally, BFD lineage delimitation analysis decisively supports a six-lineage hypothesis (Cain_Hi, Cain_Low, Divisoria, Sira, Lowland, Type) over all other lineage hypotheses, three of which include *A. smaragdina* type locality individuals constrained to be a single lineage (Table 2). Given that the *A. smaragdina* type locality individuals do not conform to a single lineage, this is strong evidence that *A. smaragdina* is not a distinct lineage. All of these results suggest that species boundaries characterized by genetic differences between *A. petersi* and *A. smaragdina* do not exist. Hereafter, mentions of *A. petersi* include populations attributed to *A. smaragdina*.

4.2. Introgression and species tree incongruence

Speciation can occur in spite of gene flow, and is more common than previously thought (Burbrink and Gehara, 2018; Mallet et al., 2016; Morales et al., 2017; Rutherford et al., 2018). Here, we used three species tree methods (SNAPP, ASTRAL-III, and TreeMix) to infer evolutionary relationships among recently-diverged populations. Two of the methods, SNAPP and ASTRAL-III, operate under the multispecies coalescent (MSC) model and consider incomplete lineage sorting (ILS) to be the sole contributor to gene tree discordance (Bryant et al., 2012; Zhang et al., 2017). We find that both methods fail to resolve nodes in the face of moderate levels of admixture, congruent with recent results from simulation and empirical studies (Solís-Lemus et al., 2016; Thom et al., 2018).

Solís-Lemus et al. (2016) found that gene tree summary methods, including the ASTRAL-III method used here, are inaccurate with moderately high levels of gene flow across the genome ($\gamma > 0.3$), although they are robust to low levels of gene flow ($\gamma < 0.1$) when a sufficient number of gene trees are used for inference. Thom et al. (2018) find similar topological inconsistencies across subspecies of an Amazonian floodplain bird species, where hybridization is supported with phenotypic and genotypic data in an intermediate subspecies. Thom et al. (2018) also find that the SNAPP topology is inconsistent with results obtained from phenotypic data and analyses that consider admixture. Both Thom et al. (2018) and Solís-Lemus et al. (2016) found improved support for a consistent species tree topology when using methods that incorporate reticulation. In this study, the two *A. petersi* populations with inconsistent topological placement across species tree analyses, Divisoria and Lowland, were also those with evidence for migration. In the sNMF analysis, there is evidence that the Lowland population admixed extensively with other *A. petersi* populations. In the TreeMix analysis, the migration edge supporting gene flow between the Divisoria population and *A. cainarachi* likely explains the Divisoria population's uncertain placement as either the sister taxon to *A. cainarachi* in the SNAPP analysis or an unresolved node in the ASTRAL analysis. The lack of statistical significance from f_3 and f_4 tests does not necessarily provide support for a lack of introgression. They may simply indicate a lack of power to detect introgression under this statistical framework, as the SNP datasets typically used for *f*-statistic analyses are two orders of magnitude larger than the present study (Reich et al., 2009).

4.3. Disturbance-vicariance and biogeography

The disturbance-vicariance (DV) hypothesis predicts that Quaternary climatic fluctuations are primarily responsible for present-day species richness and biogeographic patterns (Bush, 1994; Colinvaux, 1987). Contrary to the refugial hypothesis, which posits that allopatric refugia formed from regions of climatic stability drove speciation (Haffer, 1969), the DV hypothesis proposes that the higher diversity observed in peripheral Amazonia is due to repeated disturbance events isolating and then reconnecting populations along elevational gradients (Bush, 1994). Idiosyncratic patterns of diversification among Amazonian taxa support this hypothesis, including the exceptionally high diversity in the Andean lowlands (Bush, 1994; Noonan and Gaucher, 2006, 2005; Rull, 2008; Santos et al., 2009). Two lines of phylogeographic evidence for this hypothesis are introgression among allopatric species and structured high-elevation populations interspersed with less-structured low-elevation populations.

We provide evidence of historic introgression among two allopatric sister species, *A. petersi* and *A. cainarachi*. The introgression occurred between the ancestor of highest-elevation and northern-most sampled *A. petersi* population, the Divisoria population, which is connected to the ancestor of *A. cainarachi* by the eastern Andean foothills (Fig. 1). A probable dispersal scenario is similar to that proposed by Brown and Twomey (2009, Supplementary Fig. S4), though the results of our TreeMix analysis suggest a much simpler explanation for the recovery of weakly supported non-monophyly of *A. petersi* in the inferred species tree from SNAPP (non-monophyly was also observed by Brown and Twomey 2009 in a phylogenetic analysis of mtDNA). Brown and Twomey (2009) suggested that the speciation of *A. cainarachi* and *A. petersi* occurred shortly after another speciation event between the common ancestor of *A. cainarachi/petersi* and a third, southerly distributed daughter species. After speciation and isolation of *A. cainarachi* in the north, this third species came back into contact with ancestors of *A. petersi,* and both introgressed extensively, collapsing into a single species. Though such history remains a potential explanation for the complex speciation history of *Ameerega petersi,* our current results do not require or support the existence of a third lineage.

Our results broadly support at least one introgression event between *A. cainarachi* and *A. petersi.* We hypothesize that at least one of the species underwent cyclic population expansions and contractions (Fig. 7), which occasionally produced brief secondary contact between the two sister taxa resulting in brief, but notable, levels of introgression (Fig. 7E and G). This dynamism in distribution likely mirrored climatic dynamism, where favorable climate likely connected populations of the two species and then subsequently isolated them (Fig. 7). This may have occurred multiple times, with at least one contact event having happened (Fig. 7E and G)–as evidenced by introgression between the two species. The *A. petersi* group's preference for sloped habitats rather than flat lowlands and dependence on streams or nearby puddles for breeding also support this dispersal route hypothesis, alternative to dispersal across the lowlands (Brown, J. L., pers. obs.). Our TreeMix results detected two introgression events between the ancestor of highest-elevation and northern-most sampled *A. petersi* population, the Divisoria clade, which is connected to the ancestor of *A. cainarachi* by the eastern Andean foothills (Fig. 1). The two introgression events appear to be at different time periods and result in asymmetrical introgression from one species into the other. The two periods have signatures of introgression in opposite directions: in the one event, *A. petersi* introgressed *A. canarachi*; and in the second event, *A. cainarachi* introgressed *A. petersi*. Alternatively, this could be interpreted as a single introgression event that resulted in bi-directional introgression. Because of different population genetic histories and meta-population dynamics of either species, this produced a genomic signature of two separate events. The role of climatic dynamism and the explicit population genetic history of the *A. petersi* group is the subject of ongoing research.

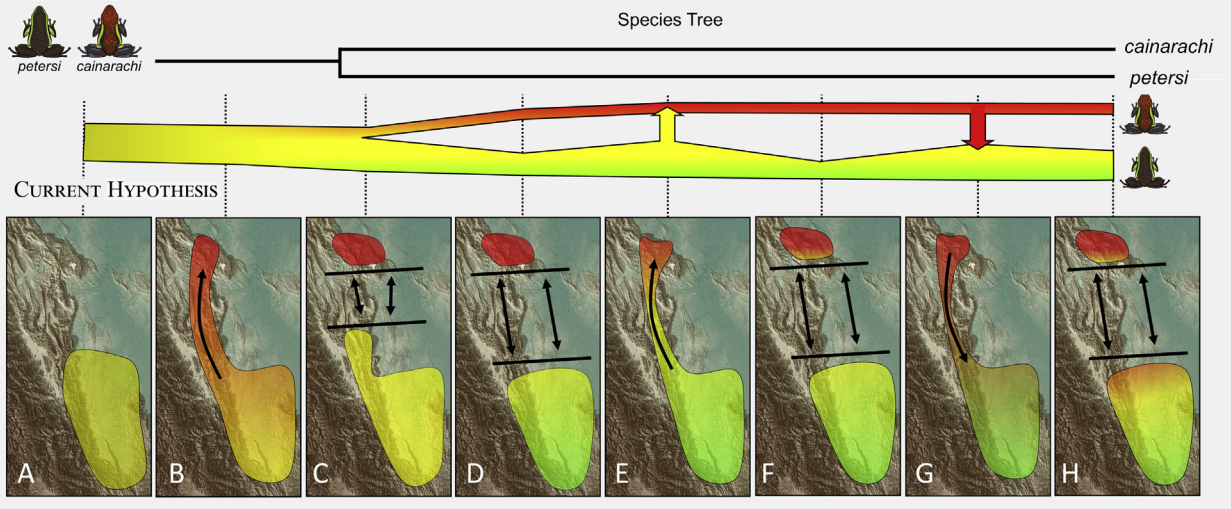

Fig. 7. Putative evolutionary history of the *Ameerega petersi* group. Our results support a biogeographic hypothesis that the ancestor to the group was (A) southern and (B) expanded north, (C) followed by subsequent isolation and speciation of *Ameerega petersi* and *A. cainarachi.* (D) After a period of isolation, which caused divergence and local structuring of populations of both species, (E) populations of each species came back into brief contact, and *A. petersi* introgressed into populations of *A. cainarachi*. (F) Following a second period of isolation, (G) populations of each species came back into brief contact, and *A. cainarachi* introgressed into populations of *A. petersi*. (H) Climate then became less suitable and both species became geographically isolated, as observed in their current distributions. Note: it is possible that E and G happened simultaneously and not as two separate events.

Preliminary phylogenetic inference supports a southerly origin of the *A. petersi* group, finding the southerly distributed *A. macero* as the sister taxon to the *A. petersi* group. This contrasts with the north-south dispersal hypothesis proposed by Roberts et al. (2006). The southerly ancestor of *A. cainarachi* and *A. petersi* then likely dispersed along the mid-elevation slopes to *A. cainarachi*'s current range. Additionally, we find that populations with lower-elevation individuals may have experienced a bottleneck followed by a recent range expansion. The Lowland and Type populations both contain individuals at the lower end of *A. petersi*'s elevational range (< 400 m). The presence of a Lowland locality at the northern tip of the Sira mountains suggests at least one recent dispersal event across the intervening lowlands separating that locality from the rest of the Lowland population. In addition, a negative Tajima's D score and low Roza's R_2 point towards a possible expansion to lower elevations after isolation. We would expect this pattern if the populations tracked habitat to higher elevations during a warming period, then expanded after conditions cooled.

5. Conclusions

We provide support for two hypotheses describing the complex speciation history of the *A. petersi* group. First, we consider *A. smaragdina* a junior synonym of *A. petersi*, with extensive behavioral and phylogenetic support. Second, admixture is present between *A. petersi* and *A. cainarachi*, likely reflecting dynamic range histories among the two species. Dynamic range histories are also reflected by non-equilibrium demographic histories in southerly-distributed *A. petersi* populations. These non-equilibrium demographic histories likely are a product of a population bottleneck followed by rapid range expansion among populations of *A. petersi*. Both admixture and non-equilibrium demographic histories support the disturbance-vicariance hypothesis as an explanation for the *A. petersi* group's speciation in the Andean foothills. Lastly, our study demonstrates the utility of UCEs as genome-wide markers for resolving shallow-scale evolutionary relationships. At shallow scales, admixture is expected to be common, and using species tree methods that also estimate admixture is important in characterizing the evolutionary history of recently-diverged species living in a heterogeneous environment. The most significant result to emerge from this study is how a simple introgression event can dramatically challenge phylogenetic inferences. Based on natural history, we have strong evidence of two species. However, due to historic introgression, some phylogenetic methods concluded the specific diversity is much higher. This study unequivocally highlights tremendous value of a detailed understanding of the focal species in their natural habitats, and without such, we could have easily concluded in favor of cryptic diversity and promoted future taxonomic confusion.

Declaration of Competing Interest

None.

Acknowledgements

We thank the Centro de Ornitología y Biodiversidad (CORBIDI) and Evan Twomey for providing tissues; Alessandro Catenazzi, Matt R. Whiles, and Alexander Shepack for helpful revisions and advice on earlier versions of this manuscript; and Kevin Horn for advice on analyses. This research was supported by start-up to Jason Brown provided by SIU. Permits to conduct field work and to export materials were issued by Peruvian authorities: INRENA (N° 002765-AG-INRENA, N° 061-2003-INRENA-IFFS-DCB, N° 050-2006-INRENA-IFFS-DCB, and N° 067-2007-INRENA-IFFS-DCB) and SERFOR (N° 083-2017-SERFOR/DGGSPFFS).

Appendix A. Supplementary material

Supplementary data to this article can be found online at https://doi.org/10.1016/j.ympev.2019.05.021.

References

Aichinger, M., 1987. Annual activity patterns of anurans in a seasonal Neotropical environment. Oecologia 71, 583–592. https://doi.org/10.1007/BF00379302.
Aichinger, M., 1991. A new species of poison-dart frog (Anura: Dendrobatidae) from the Serranía de Sira, Peru. Herpetologica 47, 1–5.
Aichinger, M., 1992. Fedundity and breeding sites of an anuran community in a seasonal tropical environment. Stud. Neotrop. Fauna Environ. 27, 9–18. https://doi.org/10.1080/01650529209360863.
Amézquita, A., Flechas, S.V., Lima, A.P., Gasser, H., Hödl, W., 2011. Acoustic interference and recognition space within a complex assemblage of dendrobatid frogs. Proc. Natl. Acad. Sci. USA 108, 17058–17063. https://doi.org/10.1073/pnas.1104773108.
Andermann, T., Fernandes, A.M., Olsson, U., Töpel, M., Pfeil, B., Oxelman, B., Aleixo, A., Faircloth, B.C., Antonelli, A., 2018. Allele phasing greatly improves the phylogenetic

utility of ultraconserved elements. Syst. Biol. https://doi.org/10.1093/sysbio/syy039.
Antonelli, A., Zizka, A., Carvalho, F.A., Scharn, R., Bacon, C.D., Silvestro, D., Condamine, F.L., 2018. Amazonia is the primary source of Neotropical biodiversity. Proc. Natl. Acad. Sci. 201713819. https://doi.org/10.1073/pnas.1713819115.
Bauer, L., 1988. Pijlgifkikkers en verwanten: de familie Dendrobatidae. Het Paludarium 1, 1–6.
Bioacoustics Research Program, 2014. Raven Pro: Interactive Sound Analysis Software (Version 1.5) [Computer software]. Ithaca, NY: The Cornell Lab of Ornithology. Available from < http://www.birds.cornell.edu/raven > .
Boul, K.E., Funk, W.C., Darst, C.R., Cannatella, D.C., Ryan, M.J., 2007. Sexual selection drives speciation in an Amazonian frog. Proc. R. Soc. Lond. B Biol. Sci. 274, 399–406. https://doi.org/10.1098/rspb.2006.3736.
Brown, J.L, Siu Ting, K., 2016. Ameerega cainarachi species account. In: Kahn, T.R., La Marca, E., Lötters, S., Brown, J.L., Twomey, E., Amézquita, A., Rodríguez-Mahecha, J. V., Mittermeier, R.A., Rylands, A.B., 2016. Aposematic poison frogs (Dendrobatidae) of the Andean countries: Bolivia, Colombia, Ecuador, Perú and Venezuela. Conservation International. pp. 142–146.
Brown, J.L., Twomey, E., 2009. Complicated histories: three new species of poison frogs of the genus *Ameerega* (Anura: Dendrobatidae) from north-central Peru. Zootaxa 2049, 1–38.
Bryant, D., Bouckaert, R., Felsenstein, J., Rosenberg, N.A., RoyChoudhury, A., 2012. Inferring species trees directly from biallelic genetic markers: bypassing gene trees in a full coalescent analysis. Mol. Biol. Evol. 29, 1917–1932. https://doi.org/10.1093/molbev/mss086.
Burbrink, F.T., Gehara, M., 2018. The biogeography of deep time phylogenetic reticulation. Syst. Biol. 67, 743–755. https://doi.org/10.1093/sysbio/syy019.
Bush, M.B., 1994. Amazonian speciation: a necessarily complex model. J. Biogeogr. 21, 5–17. https://doi.org/10.2307/2845600.
Cavalli-Sforza, L.L., Edwards, A.W.F., 1967. Phylogenetic analysis: models and estimation procedures. Evolution 21, 550–570. https://doi.org/10.1111/j.1558-5646.1967.tb03411.x.
Chazot, N., Willmott, K.R., Condamine, F.L., de-Silva, D.L., Freitas, A.V.L., Lamas, G., Morlon, H., Giraldo, C.E., Jiggins, C.D., Joron, M., Mallet, J., Uribe, S., Elias, M., 2016. Into the Andes: multiple independent colonizations drive montane diversity in the Neotropical clearwing butterflies Godyridina. Mol. Ecol. https://doi.org/10.1111/mec.13773.
Cheng, H., Sinha, A., Cruz, F.W., Wang, X., Edwards, R.L., d'Horta, F.M., Ribas, C.C., Vuille, M., Stott, L.D., Auler, A.S., 2013. Climate change patterns in Amazonia and biodiversity. Nat. Commun. 4, ncomms2415. https://doi.org/10.1038/ncomms2415.
Cochran, D.M., Goin, C.J., 1970. Frogs of Colombia. Bull. U.S. Nat. Mus. 288. pp. 19. https://doi.org/10.5962/bhl.part.6346.
Colinvaux, P., 1987. Amazon diversity in light of the paleoecological record. Quat. Sci. Rev. 6, 93–114. https://doi.org/10.1016/0277-3791(87)90028-X.
Colinvaux, P.A., 1993. Pleistocene biogeography and diversity in tropical forest of South America. In: Biological relationships between Africa and South America: Yale University Press, pp. 473–499.
Danecek, P., Auton, A., Abecasis, G., Albers, C.A., Banks, E., DePristo, M.A., Handsaker, R.E., Lunter, G., Marth, G.T., Sherry, S.T., McVean, G., Durbin, R., 2011. The variant call format and VCFtools. Bioinformatics 27, 2156–2158. https://doi.org/10.1093/bioinformatics/btr330.
Duellman, W.E., Toft, C.A., 1979. Anurans from Serranía de Sira, Amazonian Perú: taxonomy and biogeography. Herpetologica 35, 60–70.
Faircloth, B.C., 2016. PHYLUCE is a software package for the analysis of conserved genomic loci. Bioinformatics 32, 786–788. https://doi.org/10.1093/bioinformatics/btv646.
Faircloth, B.C., McCormack, J.E., Crawford, N.G., Harvey, M.G., Brumfield, R.T., Glenn, T.C., 2012. Ultraconserved elements anchor thousands of genetic markers spanning multiple evolutionary timescales. Syst. Biol. 61, 717–726. https://doi.org/10.1093/sysbio/sys004.
Frichot, E., Mathieu, F., Trouillon, T., Bouchard, G., François, O., 2014. Fast and efficient estimation of individual ancestry coefficients. Genetics 196, 973–983. https://doi.org/10.1534/genetics.113.160572.
Frost, D.R., Grant, T., Faivovich, J., Bain, R.H., Haas, A., Haddad, C.F., De Sá, R.O., Channing, A., Wilkinson, M., Donnellan, S.C., Raxworthy, C.J., Campbell, J.A., Blotto, B.L., Moler, P., Drewes, R.C., Nussbaum, R.A., Lynch, J.D., Green, D.M., Wheeler, W.C., 2006. The amphibian tree of life. Bull. Am. Mus. Nat. Hist. 1–291. https://doi.org/10.1206/0003-0090(2006) 297[0001:TATOL]2.0.CO;2.
Garzón-Orduña, I.J., Benetti-Longhini, J.E., Brower, A.V.Z., 2014. Timing the diversification of the Amazonian biota: butterfly divergences are consistent with Pleistocene refugia. J. Biogeogr. 41, 1631–1638. https://doi.org/10.1111/jbi.12330.
Grabherr, M.G., Haas, B.J., Yassour, M., Levin, J.Z., Thompson, D.A., Amit, I., Adiconis, X., Fan, L., Raychowdhury, R., Zeng, Q., Chen, Z., Mauceli, E., Hacohen, N., Gnirke, A., Rhind, N., di Palma, F., Birren, B.W., Nusbaum, C., Lindblad-Toh, K., Friedman, N., Regev, A., 2011. Trinity: reconstructing a full-length transcriptome without a genome from RNA-Seq data. Nat. Biotechnol. 29, 644–652. https://doi.org/10.1038/nbt.1883.
Grant, T., Frost, D.R., Caldwell, J.P., Gagliardo, R., Haddad, C.F.B., Kok, P.J.R., Means, D.B., Noonan, B.P., Schargel, W.E., Wheeler, W., 2006. Phylogenetic systematics of dart-poison frogs and their relatives (Amphibia, Athesphatanura, Dendrobatidae). Bull. AMNH 299. https://doi.org/10.1206/0003-0090(2006) 299[1:PSODFA]2.0.CO;2.
Grant, T., Rada, M., Anganoy-Criollo, M., Batista, A., Dias, P.H., Jeckel, A.M., Machado, D.J., Rueda-Almonacid, J.V., 2017. Phylogenetic systematics of dart-poison frogs and their relatives revisited (Anura: Dendrobatoidea). South Am. J. Herpetol. 12, S1–S90. https://doi.org/10.2994/SAJH-D-17-00017.1.
Guindon, S., Dufayard, J.-F., Lefort, V., Anisimova, M., Hordijk, W., Gascuel, O., 2010. New algorithms and methods to estimate maximum-likelihood phylogenies: assessing the performance of PhyML 3.0. Syst. Biol. 59, 307–321. https://doi.org/10.1093/sysbio/syq010.
Haffer, J., 1969. Speciation in Amazonian forest birds. Science 165, 131–137. https://doi.org/10.1126/science.165.3889.131.
Harvey, M.G., Smith, B.T., Glenn, T.C., Faircloth, B.C., Brumfield, R.T., 2016. Sequence capture versus restriction site associated DNA sequencing for shallow systematics. Syst. Biol. 65, 910–924. https://doi.org/10.1093/sysbio/syw036.
Hoang, D.T., Chernomor, O., von Haeseler, A., Minh, B.Q., Vinh, L.S., 2018. UFBoot2: improving the ultrafast bootstrap approximation. Mol. Biol. Evol. 35, 518–522. https://doi.org/10.1093/molbev/msx281.
Hödl, W., 1990. Reproductive diversity in Amazonian lowland frogs. Fortschr. Zool. 38, 41–60.
Hoorn, C., Wesselingh, F.P., Steege, H., Bermudez, M.A., Mora, A., Sevink, J., Sanmartín, I., Sanchez-Meseguer, A., Anderson, C.L., Figueiredo, J.P., Jaramillo, C., Riff, D., Negri, F.R., Hooghiemstra, H., Lundberg, J., Stadler, T., Särkinen, T., Antonelli, A., 2010. Amazonia through time: Andean uplift, climate change, landscape evolution, and biodiversity. Science 330, 927–931. https://doi.org/10.1126/science.1194585.
Hosner, P.A., Faircloth, B.C., Glenn, T.C., Braun, E.L., Kimball, R.T., 2016. Avoiding missing data biases in phylogenomic inference: an empirical study in the landfowl (Aves: Galliformes). Mol. Biol. Evol. 33, 1110–1125. https://doi.org/10.1093/molbev/msv347.
Hudson, R.R., 2002. Generating samples under a Wright-Fisher neutral model of genetic variation. Bioinformatics 18, 337–338. https://doi.org/10.1093/bioinformatics/18.2.337.
Jombart, T., 2008. adegenet: a R package for the multivariate analysis of genetic markers. Bioinformatics 24, 1403–1405. https://doi.org/10.1093/bioinformatics/btn129.
Jombart, T., Ahmed, I., 2011. adegenet 1.3-1: new tools for the analysis of genome-wide SNP data. Bioinformatics 27, 3070–3071. https://doi.org/10.1093/bioinformatics/btr521.
Kalyaanamoorthy, S., Minh, B.Q., Wong, T.K.F., von Haeseler, A., Jermiin, L.S., 2017. ModelFinder: fast model selection for accurate phylogenetic estimates. Nat. Methods 14, 587–589. https://doi.org/10.1038/nmeth.4285.
Katoh, K., Standley, D.M., 2013. MAFFT multiple sequence alignment software version 7: improvements in performance and usability. Mol. Biol. Evol. 30, 772–780. https://doi.org/10.1093/molbev/mst010.
Leaché, A.D., Fujita, M.K., Minin, V.N., Bouckaert, R.R., 2014. Species delimitation using genome-wide SNP data. Syst. Biol. 63, 534–542. https://doi.org/10.1093/sysbio/syu018.
Lemmon, E.M., 2009. Diversification of conspecific signals in sympatry: geographic overlap drives multidimensional reproductive character displacement in frogs. Evolution 63, 1155–1170. https://doi.org/10.1111/j.1558-5646.2009.00650.x.
Li, H., Durbin, R., 2009. Fast and accurate short read alignment with Burrows-Wheeler transform. Bioinforma. Oxf. Engl. 25, 1754–1760. https://doi.org/10.1093/bioinformatics/btp324.
Li, H., Handsaker, B., Wysoker, A., Fennell, T., Ruan, J., Homer, N., Marth, G., Abecasis, G., Durbin, R., 1000 Genome Project Data Processing Subgroup, 2009. The Sequence Alignment/Map format and SAMtools. Bioinforma. Oxf. Engl. 25, 2078–2079. https://doi.org/10.1093/bioinformatics/btp352.
Liou, L.W., Price, T.D., 1994. Speciation by reinforcement of premating Iiolation. Evolution 48, 1451–1459. https://doi.org/10.1111/j.1558-5646.1994.tb02187.x.
Lötters, S., Reichle, S., Jungfer, K.-H., 2003. Advertisement calls of Neotropical poison frogs (Amphibia: Dendrobatidae) of the genera *Colostethus, Dendrobates* and *Epipedobates,* with notes on dendrobatid call classification. J. Nat. Hist. 37, 1899–1911. https://doi.org/10.1080/00222930110089157.
Lötters, S., Mutschmann, F., 2007. Poison frogs: biology, species and captive care. Edition Chimaira, Frankfurt, Germany.
Mallet, J., Besansky, N., Hahn, M.W., 2016. How reticulated are species? BioEssays 38, 140–149. https://doi.org/10.1002/bies.201500149.
Manthey, J.D., Campillo, L.C., Burns, K.J., Moyle, R.G., 2016. Comparison of target-capture and restriction-site associated DNA sequencing for phylogenomics: a test in cardinalid tanagers (Aves, Genus: *Piranga*). Syst. Biol. 65, 640–650. https://doi.org/10.1093/sysbio/syw005.
McKenna, A., Hanna, M., Banks, E., Sivachenko, A., Cibulskis, K., Kernytsky, A., Garimella, K., Altshuler, D., Gabriel, S., Daly, M., DePristo, M.A., 2010. The Genome Analysis Toolkit: a MapReduce framework for analyzing next-generation DNA sequencing data. Genome Res. 20, 1297–1303. https://doi.org/10.1101/gr.107524.110.
Morales, A.E., Jackson, N.D., Dewey, T.A., O'Meara, B.C., Carstens, B.C., 2017. Speciation with gene flow in North American *Myotis* bats. Syst. Biol. 66, 440–452. https://doi.org/10.1093/sysbio/syw100.
Myers, C.W., Daly, J.W., Malkin, B., 1978. A dangerously toxic new frog (*Phyllobates*) used by Emberá Indians of western Colombia, with discussion of blowgun fabrication and dart poisoning. Bull. Am. Mus. Nat. Hist. 161, 307–366.
Myers, C.W., 1982. Spotted poison frogs: descriptions of three new *Dendrobates* from western Amazonia, and resurrection of a lost species from "Chiriqui". Am. Museum Novit. 272, 1–23.
Myers, C.W., 1987. New generic names for some neotropical poison frogs (Dendrobatidae). Pap. Avulsos Zool. 36, 301–306.
Myers, C.W., Rodríguez, L.O., Icochea, J., 1998. *Epipedobates simulans*, a new cryptic species of poison frog from southeastern Peru, with notes on *E. macero* and *E. petersi* (Dendrobatidae). Am. Museum Novit 3238.
Myers, N., Mittermeier, R.A., Mittermeier, C.G., da Fonseca, G.A.B., Kent, J., 2000. Biodiversity hotspots for conservation priorities. Nature 403, 853–858. https://doi.org/10.1038/35002501.

Nguyen, L.-T., Schmidt, H.A., von Haeseler, A., Minh, B.Q., 2015. IQ-TREE: a fast and effective stochastic algorithm for estimating maximum-likelihood phylogenies. Mol. Biol. Evol. 32, 268–274. https://doi.org/10.103/molbev/msu300.

Noonan, B.P., Gaucher, P., 2006. Refugial isolation and secondary contact in the dyeing poison frog *Dendrobates tinctorius*. Mol. Ecol. 15, 4425–4435. https://doi.org/10.1111/j.1365-294X.2006.03074.x.

Noonan, B.P., Gaucher, P., 2005. Phylogeography and demography of Guianan harlequin toads (*Atelopus*): diversification within a refuge. Mol. Ecol. 14, 3017–3031. https://doi.org/10.1111/j.1365-294X.2005.02624.x.

Pfeifer, B., Wittelsbürger, U., Ramos-Onsins, S.E., Lercher, M.J., 2014. PopGenome: an efficient Swiss army knife for population genomic analyses in R. Mol. Biol. Evol. 31, 1929–1936. https://doi.org/10.1093/molbev/msu136.

Pickrell, J.K., Pritchard, J.K., 2012. Inference of population splits and mixtures from genome-wide allele frequency data. PLOS Genet. 8, e1002967. https://doi.org/10.1371/journal.pgen.1002967.

Ramos-Onsins, S.E., Rozas, J., 2002. Statistical properties of new neutrality tests against population growth. Mol. Biol. Evol. 19, 2092–2100. https://doi.org/10.1093/oxfordjournals.molbev.a004034.

Reich, D., Thangaraj, K., Patterson, N., Price, A.L., Singh, L., 2009. Reconstructing Indian population history. Nature 461, 489–494. https://doi.org/10.1038/nature08365.

Roberts, J.L., Brown, J.L., von May, R., Arizabal, W., Schulte, R., Summers, K., 2006. Genetic divergence and speciation in lowland and montane Peruvian poison frogs. Mol. Phylogenet. Evol. 41, 149–164. https://doi.org/10.1016/j.ympev.2006.05.005.

Roberts, J.L., Brown, J.L., Schulte, R., Arizabal, W., Summers, K., 2007. Rapid diversification of colouration among populations of a poison frog isolated on sky peninsulas in the central cordilleras of Peru. J. Biogeogr. 34, 417–426. https://doi.org/10.1111/j.1365-2699.2006.01621.x.

da Rocha, D.G., Kaefer, I.L., 2019. What has become of the refugia hypothesis to explain biological diversity in Amazonia? Ecol. Evol. 312, 673. https://doi.org/10.1002/ece3.5051.

Rodríguez, L.O., Myers, C.W., 1993. A new poison frog from Manu National Park, southeastern Peru (Dendrobatidae *Epipedobates*). Am. Museum 3068.

Rojas, B., Endler, J.A., 2013. Sexual dimorphism and intra-populational colour pattern variation in the aposematic frog *Dendrobates tinctorius*. Evol. Ecol. 27, 739–753. https://doi.org/10.1007/s10682-013-9640-4.

Rull, V., 2008. Speciation timing and neotropical biodiversity: the Tertiary-Quaternary debate in the light of molecular phylogenetic evidence. Mol. Ecol. 17, 2722–2729. https://doi.org/10.1111/j.1365-294X.2008.03789.x.

Rutherford, S., Rossetto, M., Bragg, J.G., McPherson, H., Benson, D., Bonser, S.P., Wilson, P.G., 2018. Speciation in the presence of gene flow: population genomics of closely related and diverging Eucalyptus species. Heredity 1. https://doi.org/10.1038/s41437-018-0073-2.

Santos, J.C., Coloma, L.A., Summers, K., Caldwell, J.P., Ree, R., Cannatella, D.C., 2009. Amazonian amphibian diversity is primarily derived from late Miocene Andean lineages. PLOS Biol. 7, e1000056. https://doi.org/10.1371/journal.pbio.1000056.

Sayyari, E., Mirarab, S., 2016. Fast coalescent-based computation of local branch support from quartet frequencies. Mol. Biol. Evol. 33, 1654–1668. https://doi.org/10.1093/molbev/msw079.

Schlüter, A., 1980. Bio-akustische Untersuchungen an Dendrobatiden in einem begrenzten Gebiet des tropischen Regenwaldes von Peru. Salamandra 16, 149–161.

Serrano-Rojas, S.J., Whitworth, A., Villacampa, J., Von May, R., Padial, J.M., Chaparro, J.C., 2017. A new species of poison-dart frog (Anura: Dendrobatidae) from Manu province, Amazon region of southeastern Peru, with notes on its natural history, bioacoustics, phylogenetics, and recommended conservation status. Zootaxa 4221, 071–094. https://doi.org/10.11646/zootaxa.4221.1.3.

Silverstone, P.A., 1976. A revision of the poison-arrow frogs of the genus *Phyllobates* Bibron in Sagra (Family Dendrobatidae). Nat Hist. Mus. Los Angeles Cty. Sci. Bull. 27, 1–50.

Solís-Lemus, C., Yang, M., Ané, C., 2016. Inconsistency of species tree methods under gene flow. Syst. Biol. 65, 843–851. https://doi.org/10.1093/sysbio/syw030.

Tajima, F., 1989. Statistical method for testing the neutral mutation hypothesis by DNA polymorphism. Genetics 123, 585–595.

Thom, G., Amaral, F.R.D., Hickerson, M.J., Aleixo, A., Araujo-Silva, L.E., Ribas, C.C., Choueri, E., Miyaki, C.Y., 2018. Phenotypic and genetic structure support gene flow generating gene tree discordances in an Amazonian floodplain endemic species. Syst. Biol. https://doi.org/10.1093/sysbio/syy004.

Toft, C.A., 1980. Feeding ecology of thirteen syntopic species of anurans in a seasonal tropical environment. Oecologia 45, 131–141. https://doi.org/10.1007/BF00346717.

Toft, C.A., Duellman, W.E., 1979. Anurans of the lower Río Llullapichis, Amazonian Perú: a preliminary analysis of community structure. Herpetologica 35, 71–77.

Turchetto-Zolet, A.C., Pinheiro, F., Salgueiro, F., Palma-Silva, C., 2013. Phylogeographical patterns shed light on evolutionary process in South America. Mol. Ecol. 22, 1193–1213. https://doi.org/10.1111/mec.12164.

Twomey, E., Vestergaard, J.S., Venegas, P.J., Summers, K., 2016. Mimetic divergence and the speciation continuum in the Mimic Poison Frog *Ranitomeya imitator*. Am. Nat. 187, 205–224. https://doi.org/10.1086/684439.

Watterson, G.A., 1975. On the number of segregating sites in genetical models without recombination. Theor. Popul. Biol. 7, 256–276. https://doi.org/10.1016/0040-5809(75)90020-9.

Weygoldt, P., 1987. Evolution of parental care in dart poison frogs (Amphibia: Anura: Dendrobatidae). J. Zoolog. Syst. Evol. Res. 25, 51–67.

Zhang, C., Sayyari, E., Mirarab, S., 2017. ASTRAL-III: increased scalability and impacts of contracting low support branches, in: Comparative genomics, lecture notes in computer science. Presented at the RECOMB international workshop on comparative genomics, Springer, Cham, pp. 53–75. https://doi.org/10.1007/978-3-319-67979-2_4.